SPRING-NEAP TIDAL PATTERNS IN NORTH ATLANTIC TROPICAL CYCLONES

Peter H. Yaukey[*]

University of New Orleans, New Orleans, USA

ABSTRACT

Tropical cyclones are hypothesized to reduce their own intensity by mixing of cool water upward, locally reducing the warmth of the sea surface. Little is known about how temperature variations in subsurface waters might moderate their influence on cyclones over sub-seasonal time scales. For instance, cold water might be mixed upward to depths accessible to storms by internal tidal waves (bores) propagated along the thermocline. I explored the possible influence of tidal mixing on near-surface ocean temperature profiles and tropical cyclones by analyzing patterns of cyclone frequency and intensity, and of subsurface water temperatures, across the spring-neap tidal cycle.

_____

[*]_Corresponding author address:_ Department of Geography, University of New Orleans, New Orleans, LA, USA, 70148; e-mail: pyaukey@uno.edu.

Atlantic best-track observations from 1950-2007 displayed a pronounced peak of both hurricane occurrence and mean cyclone wind speed half way between the new and full moon. These patterns were consistent over time, being correlated between the first (1950-1978) and second (1979-2007) halves of the study period. This pattern of hurricane occurrence was similar east and west of 55^0W and in the Gulf of Mexico/Caribbean Sea, but appeared phase shifted by ~7 d north of 35^0N. Initiation dates of rapid intensification events (≥15 kt increase in 24 h) were distributed non-uniformly across the synodic cycle, and showed peaks more directly centered on the new (major peak) and full moon (minor).

Water temperatures at 35-150m depth at three long term moorings between 12^0N and 32^0N were each dominated by a peak near

1

the new moon, matching the timing of intensification events, although they varied in other details. Within 500 km of the 12^0N and 15^0N moorings, cyclones that passed while rapidly intensifying appeared to be associated with warmer 35-150m waters than were other passing cyclones. Evidence less consistent with tidal influence include the presence of a relatively strong lunar pattern in hurricane occurrence in the Gulf of Mexico and Caribbean Sea where tides are weak, the limited amplitude of spring-neap temperature variations (only 0.1-0.2^0C) and their inconsistency across years at two of the mooring sites.

KEY WORDS: Tropical cyclone; hurricane; rapid intensification; tidal; spring-neap.

1. INTRODUCTION

Forecasting of hurricane intensity remains an important challenge for tropical cyclone researchers. Accurate intensity forecasting is critical to warning coastal communities of the level of threat posed by approaching storms, yet advances in forecasting intensity have not kept pace with those in predicting of storm tracks, with especially large errors in the realm of rapid intensification (Rappaport *et al.*, 2009). The National Hurricane Center has elevated improvements in intensity forecasting to their top priority for tropical meteorology research. Intensification of hurricanes is widely recognized to be affected by a variety of factors, including vertical wind shear, humidity, vorticity, and upper-level divergence. Ocean temperature is critical to storm intensification, including not just surface temperature but also the depth of the surface layer of warm water (Hong *et al.*, 2000; Mao *et al.*, 2000; Shay *et al.,* 2000; Gino and Trinanes, 2003).

The heat content of the uppermost ocean and variation of water temperature with depth near the surface depend upon several factors, such as the presence and depth of warm ocean currents and eddies, radiant fluxes, and wind. In recent years oceanographers have also become aware that much more tidal energy dissipation occurs away from the continental shelves than was previously thought (Egbert and Ray, 2000; Garrett, 2003; Jayne, 2005; Thorpe, 2005). The ability of tidal movements to

induce mixing of water near the ocean surface is still not well understood, but mixing in the upper ocean has been reported from modeling and empirical studies both far from (e.g., Martin, 2007; Schiller and Fiedler, 2007) and along continental shelves (e.g., Creswell and Badcock, 2000; Sharples et al., 2006). Deep ocean tidal mixing is thought to be generated at seafloor topographic features, and it is not clear how far tidal energy can spread from these. One possible mechanism of spread is via movements of internal waves along the thermocline. Such internal waves create predictable upwelling and surface cooling with fortnightly periodicity, at least at several locations on the Pacific Coast of North America (Pineda 1991, 1995). At present, tidal variations in subsurface water temperatures are not incorporated into cyclone forecasting.

The purpose of this paper is investigate whether the subsurface waters within reach of wind-induced mixing by passing cyclones exhibit meaningful temporal variation on the spring-neap tidal cycle, which might indicate the potential to influence cyclone intensification. I begin by examining variations in the occurrence and intensity of tropical cyclones across the spring-neap cycle. I then examine temperature fluctuations down to 150m at three long term moorings in the Atlantic, to assess whether sub-surface temperatures vary in a pattern consistent with patterns exhibited by the cyclones. I focus on the Atlantic basin, where the most complete and precise historical database of storm wind speeds is available.

2. METHODS

2.1 Tropical cyclone records

I obtained tropical cyclone records at 6 h intervals from June-November between 1950 and 2007 from the best track analyses of the National Hurricane Center's North Atlantic Hurricane Database (HURDAT, http://www.nhc.noaa.gov/pastatll.shtml).

Records prior to 1950 were excluded because most lacked data from the early (tropical depression) phase of storm development, and observations made north of 50^0N or coded as "extratropical" were omitted. The onset of rapid intensification was identified for storms that experienced a Rapid Intensification Event (RIE) of ≥15 knots

(7.7 ms^{-1}) over 24 h. Intensification calculations did not begin until a storm was classified as a tropical or subtropical system of at least depression strength, and consecutive (beginning 6 h after another ended) or overlapping RIE were considered a single event. When a storm had more than one RIE, that with the largest total wind speed increase was used; maximum 6 h increase within the RIE was the second tie breaker. To exclude RIEs caused merely by landfall-weakened storms intensifying as they returned to sea, post-landfall RIE did not begin until storms had regained their pre-landfall strength. If this happened in between observations, the storm was assumed to have regained it at the midpoint in between those observations. Pre-landfall wind speed was taken from the last observation before the official track came ashore. For purposes other than RIE, observations within 3 d after being over land (coded as 1^0 x 1^0 blocks that intersected land) were excluded. For all purposes, only contacts with a continental mainland or Greater Antillean island constituted landfall. Identification of RIE and landfalls in HURDAT was assisted by individual storm accounts in the National Hurricane Center online archives, and storm track maps on the UNISYS website (www.weather.unisys.com/hurricane).

2.2 Ocean temperature

Three moorings that have especially lengthy records of sub-surface temperatures in cyclone-prone areas of the Atlantic were selected for analysis (Fig. 1). Two were adjacent components of the PIRATA array located at 12.0^{0}N 38.0^{0}N and 15.0^{0}N 38.0^{0}N, 333 km apart (available at http://www.pmel.noaa.gov/tao/data_deliv/deliv-nojava-pir.html). Daily temperature readings were available from these moorings back to 1999 and 1998 respectively, at 20 m depth intervals down to 140 m and at 180m. For days that were missing data from a single depth or two adjacent depths that were bounded by measurements 20m above and below, missing temperatures were filled in by interpolation between the next deeper and shallower values, based simply on the mean relative magnitude of the missing depth's temperature between its two bounding depths

4

in the overall data set. Days with more missing data were omitted

The third mooring, the Bermuda Testbed site (31.7^{0}N 64.2^{0}W), has been operating since 1994 (data available at http://www.opl.ucsb.edu/btm.html). Sensor depths here have shifted over time and this analysis will focus on the four depths that offer the greatest number of observations since the mooring began: 3, 35, 70, and 150 m. The sensor depths used actually varied around each of these targets by as much as 1m (for the 3m depth), 5m (for 35m and 70m), or 9m (for 150m). When more than one sensor was available at a given depth, only one was used- generally the Tidbit sensor because of its wide availability over the series of moorings.

2.3 Spring-neap tidal cycle

I matched storm and mooring observations to the spring-neap (lunar phase) cycle by calculating the time elapsed from the preceding full moon to the hour of observation, divided by the time span between that full moon and the subsequent full moon (i.e., the "synodic decimal"). Serial correlation among successive temperature or

HURDAT observations posed challenges for testing for statistical significance. I dealt with this problem in two ways. First, I compared patterns of cyclone occurrence and wind speed or ocean water temperature on the lunar cycle between the years in the first and second halves of the study period (1950-1978, 1979-2007 for cyclones) using simple correlation; correlated patterns were considered unlikely to be spurious. For this purpose, each synodic cycle was partitioned into 30 equal "days" (cf. mean length of 29.53 d) and the frequency of hurricane observations, mean wind speed, or mean water temperature was calculated for each synodic day. To prevent complications from arising due to the slightly shorter length of synodic than calendar days, temperatures were first calculated as 24 h means before each was assigned to its synodic day (at 12Z). For cyclones I assumed that the 57 yr span of cyclone observations was sufficiently long (>280 synodic cycles) to prevent spurious patterns from arising because of repeated chance alignments of the same portions of the synodic cycle with storm observations made at particular times of day;

5

for instance, in infrequent cases synodic days spanned only 3 not 4 HURDAT observations. Analysis of the samples supported this assumption: the four observation times had approximately equal representation on each synodic day, each accounting for between 22.8%-27.3% of the observations.

Second, I reduced the data set to a single observation (the starting point of the RIE) from each storm, and tested these for non-uniformity across the lunar cycle using Watson's U^2 test (*Zar*, 1984), a nonparametric test for circular data that employs rankings of observations:

$$U^2 = \sum u_i^2 - (\sum u_i^2)/n - (2/n)(\sum i u_i) +$$
$$(n + 1)\bar{u} + n/12$$

where u is the synodic decimal of a given cyclone or temperature observation.

3. RESULTS

3.1 Distribution of hurricanes and cyclone wind speeds across the spring-neap tidal cycle

Removal of HURDAT observations outside June-November or within 3 d after being over land left 12,429 observations, of which 4490 were of hurricanes (wind speed ≥

32.4 ms^{-1}). I partitioned the lunar month (29.53 d) into 30 equal intervals, or synodic "days." A dominant peak in the occurrence of hurricane observations existed half way between the new and full moon (Fig 2), with 224 hurricane observations on day 24 (vs. a low of 110 on day 10). The distribution of observations of hurricanes among the 30 days of the spring-neap cycle appear similar in the first (1950-1978) and second (1979-2007) halves of the study period, and are correlated (r = 0.61, P =0.0003; Fig 2). Systems with sub-hurricane wind speeds also show a single dominant peak, shifted nearly a week earlier on the cycle (Fig 3).

Mean wind speeds of tropical systems (of all strengths) also showed a peak approximately half way from the new to the full moon; mean speeds ranged from 93.9 kph (26.1 ms^{-1}) on days 13 and 18 to 115.7 kph (32.1 ms^{-1}) on day 23 (Fig 4). The distribution of mean wind speeds among synodic days was correlated between the first and second halves of the study period (r = 0.46, n = 30, P = 0.0099; Fig 4).

To examine geographical variation, I used all tropical cyclones, including

depressions, to boost the sample size to accommodate geographical subdivision. The three regions below 35^0N showed a consistent pattern in cyclone occurrence, dominated by a new-moon peak (Fig 5). Tropical cyclones above the 35th parallel appear to be phase shifted from these by ~7d. Exploratory movement of this latitudinal boundary (in units of 5^0) indicated that splitting the Atlantic at 35^0N produced the most concise change of pattern. After being smoothed by a 5d running mean, the amplitude of the peaks and troughs of the four distributions was similar: peak daily means were 63% higher than lows in all regions except the southwestern open Atlantic, where they differed by 79%. Thus, the Gulf of Mexico and Caribbean Sea did not show reduced lunar influence as a consequence of their limited ocean tidal fluctuations, a potential inconsistency with the tidal mixing hypothesis.

3.2 Onset of rapid intensification

A total of 534 tropical systems exhibited at least one Rapid Intensification Event (RIE) of ≥ 15 kt within a 24 h period. Twenty of these systems had two RIE, and two had three each (Jeanne and Lisa, both in 2004); the single greatest RIE was selected for each. Seventy-five systems in HURDAT had no RIE and were excluded.

RIE inceptions were distributed non-uniformly around the lunar synodic cycle (Watson's U^2 = 0.1962, N = 534, P = 0.0416; Fig. 6). RIEs were concentrated around the new moon, with a lesser concentration around the full moon. Centered on the new moon, days 11-21 averaged 21.4 RIE inceptions/day over the 58 years; all but day 15 were above the mean (17.8) of the 30 d. The seven days centered on the full moon averaged 18.1 RIE/day, and contained four of the remaining five above-average days. In contrast, the 14 days between these peak periods averaged 14.3 RIE/day. Thus, the peak period centered on the new moon averaged 49% more RIE per day than the 6-7 days on each side of it.

3.3 Distribution of sub-surface temperatures across the spring-neap tidal cycle

After graphing mean 35-150 m temperatures on the lunar synodic cycle (divided into 30 "days") and smoothing using a five day running mean, temperatures at each site were dominated by a single peak near the new moon. Maxima at all three moorings were between days 15-18. Thus, the peak in sub-surface temperature occurred during the same lunar phase as did inception of storm RIE, near the new moon. The occurrence of RIE in storms passing these moorings was also related to the sub-surface temperatures they reported at the time of closest passage: cyclones passing within 500 km of the 12^0N mooring that were experiencing RIE (n = 10) did so at times of warmer 35-150m temperatures than those not undergoing rapid intensification (n = 11), although this pattern was only marginally significant (Wilcoxon Two Sample Test, Z = 1.37, one-tailed p = 0.0849). Temperature data at the 15^0N mooring suggested the same pattern (n = 12 cyclones with RIE, 13 without RIE; Z = 0.95, p = 0.1706). These results were not just a consequence of storms having RIE during warmer times of the season; storms experiencing RIE did not

pass on days with warmer long term mean temperatures (5 day running means for each date measured over life span of mooring) than passing storms without RIE (18.3^0 vs. 18.2^0C at 12^0N, 22.4^0C for both groups at 15^0N; one-tailed p > 0.3 for both in Wilcoxon Two Sample tests).

These two Pirata sites are only 333 km apart and thus do not represent fully independent tests, and the Bermuda Testbed site could not be analyzed in this respect because only one cyclone passing within 500 km experienced rapid intensification. Also, while the 15^0N mooring showed sub-surface temperature variations across the lunar cycle that were correlated between the first and second halves of its years of record (r = 0.58, n=30, p=0.0009, using raw means vs. smoothed values), neither Bermuda Testbed (r = -0.03, n=30, p = 0.8828), nor the 12^0N site (r = 0.14, n = 30, P = 0.4601) showed consistent patterns in the first and second halves of their records. The magnitude of variations potentially created by the spring-neap cycle was low, with peaks and troughs on the smoothed graphs separated by only 0.1-0.2^0C at each site. The similarity of the

RIE distribution and the timing of peak sub-surface temperatures at all three moorings (Fig. 1) is consistent with the tidal mixing hypothesis, but the inter-annual inconsistency of these temperature patterns at two moorings, and their small magnitude, and the lack of explanation for the dominance of the new moon peak make interpretation difficult..

4. DISCUSSION

This study has documented significant variations in hurricane occurrence and cyclone wind speed with lunar phase, which have been consistent over the last half century and across the tropical and subtropical Atlantic. While hurricane occurrence and cyclone wind speed exhibited a single dominant peak half way between the new and full moons, rapid intensification events peaked more directly on the new moon. This new moon peak matched a new moon peak in subsurface ocean temperatures at each of three long term moorings, and the pair of moorings in the eastern tropical Atlantic showed marginally significant associations between subsurface

temperatures and the tendency of passing storms to rapidly intensify.

The strength of the lunar pattern in cyclone activity was greater than expected. Peak lunar days had nearly 50% more intensification events, an ~80% increase in hurricane occurrence, and a ~15 kph (4 ms^{-1}) increase in wind speed relative to the low points in the lunar cycle. Although variation of cyclone activity on the spring-neap cycle has been absent from the scientific literature in recent decades, it is not a new idea. Charles Smiley (1954) proposed that the atmospheric tide may influence hurricanes (but was criticized by *Jordan*, 1955). A decade later a more comprehensive study of Atlantic hurricanes (*Bradley*, 1964) showed a broad new moon peak and smaller full moon peak in formation dates, and another showed that formation dates of depressions (which often develop into cyclones) in the Indian Ocean near India also varied across the synodic cycle (*Visvanathan*, 1966). *Carpenter et al.* (1972) reported new moon and (smaller) full moon peaks in cyclone formation dates, in both the North Atlantic and Western Pacific. The latter study

9

reported only a ~20% increase in cyclone formations at their peak in the lunar synodic cycle. The stronger pattern found in the present study is presumably attributable to the improvements in data availability and quality in recent decades, and to the ability to now examine wind speed rather than merely storm formation dates.

Earlier studies were unable to identify the forcing mechanism(s) creating lunar variation in tropical cyclones, but emphasized the atmospheric tide, which is widely recognized as being only a weak influence in the troposphere (*American Meteorological Society,* 2009). The influence of ocean warmth on cyclones makes oceanic processes a logical place to look for an explanation, especially in light of recent discoveries revealing that large amounts of tidal energy are dissipated in the open ocean. However, the evidence presented here is not yet sufficient to conclusively identify this as a primary forcing factor. It is unclear whether the 0.1-0.2^0C variations in temperature on the spring-neap cycle are sufficient to produce substantial variations in storm intensity. The relationship of cyclone wind speed to ocean temperature remains imperfectly understood (e.g., Evans, 1993; Michaels et al., 2006). One modeling study that specifically simulated cyclones mixing upper ocean waters beneath their eye walls showed intensification to be significantly reduced by surface cooling of 1.0 C^0 and halted by cooling of 2.5 C^0 (Pasquero and Emanuel, 2008). More study is needed to determine the relationship of near-surface water temperatures to cyclone intensification in the context of storm-induced mixing.

The peak timing of intensification events at the spring tide is also puzzling, since upwelling might be expected to be greatest at that time. However, surface cooling caused by breaking of internal tidal bores along the Pacific Coast of the USA was also reported to peak at the neap tides at most sites (Pineda 1991, 1995). The dominance of the new moon peak over the full is also curious; full and new moon tidal heights along shorelines are generally similar. This new moon dominance is evident in the timing of RIE, but dominance of a single peak is even more pronounced in the timing of hurricane observations and mean wind speeds. The

simple notion that intensification progresses with the amount of time spent in favorable ocean conditions might help explain this. If the RIE distribution is taken to approximate the favorability of conditions for intensification, its short full moon peak might at times provide too few days for strong winds to develop, while the longer new moon peak may be more likely to provide sufficient time. This could cause hurricane observations or mean wind speeds to be even more heavily dominated by a single peak (after the new moon) than is RIE. This would also explain why the hurricane frequency and mean wind speed peaks are ~ 7d later than for RIE or for less intense storms.

The weakness of tides in the Gulf of Mexico and Caribbean Sea might have been expected to limit the influence of tidal processes there. To the contrary, the amplitude of the variations of hurricane occurrence with lunar phase were as large here as in the open Atlantic. This might be partially explained by the relatively large portion of this area that is close to shelf edges or other topographic complexities that could amplify tidal mixing.

While the moorings each showed a peak in temperature between day 15-18 on the lunar synodic cycle, serial correlation made it difficult to verify these patterns. Only one site showed a pattern that was significantly correlated between the first and second halves of the mooring temperature record. Unfortunately, long term subsurface temperature data at consistent locations are scarce (*Swain et al.*, 2006). Altimeter readings are used to estimate the depth of the surface mixed layer (*Gino and Trinanes*, 2003), but the ability of altimeter readings to resolve events of upward mixing of cold water into the thermocline area from below need to be resolved. Analysis of additional mooring sites may not be productive until several years pass and allow more data to accumulate at additional sites. Data that are more central to the areas of most frequent tropical cyclone intensification would be especially valuable. Further study of the relationship of tidal processes to tropical cyclones is important, given the potential benefit that the predictability of tidal processes would confer to cyclone forecasting. Additional analyses in the

Pacific and Indian Oceans would provide valuable insight, as well as detailed examinations of the influence of subsurface ocean temperatures on individual storms.

REFERENCES

American Meteorological Society. 2009: Lunar atmospheric tide. Glossary of Meteorology, 2nd ed. http://amsglossary.allenpress.com/glossary. Accessed 22 June 2009.

Bradley D., 1964: Tidal components in hurricane development. *Nature,* **204,** 136–138.

Carpenter et al., 1972: Observed relationships between lunar tidal cycles and the formation of hurricanes and tropical storms. *Mon. Weath. Rev.,* **100,** 451-460.

Cresswell G.R., Badcock, K.A., 2000: Tidal mixing near the Kimberley coast of NW Australia, *Marine and Freshwater Researc,.* **5,** 641 – 646.

Egbert G.D., Ray R.D., 2000: Significant dissipation of tidal energy in the deep ocean inferred from satellite altimeter data. *Nature,* **405,** 775-778.

Evans, J., 1993: Sensitivity of tropical cyclone intensity to sea surface temperature. *J. Climate,* **6,** 1133-1140.

Garrett, C., 2003: Enhanced internal tides and ocean mixing. *Science,* **301,** 1858 – 1859.

Gino, G.J., and Trinanes, J.A., 2003: Ocean thermal structure monitoring could aid in the intensity forecast of tropical cyclones. *Eos,* **84,** 573-580.

Hong, X., Chang, S.W., Raman, S., Shay, L.K., and Hodur, R., 2000: The interaction between Hurricane Opal (1995) and a warm core ring in the Gulf of Mexico. *Mon. Wea. Rev.,* **128,** 1347–1365.

Jayne, S.R. 2005: Ocean Topography, Tides, Mixing, and the Earth's Climate. *Oceans,* **2005,** 1-4.

Jordan C., 1955: Tidal forces and the formation of hurricanes. *Nature,* **175,** 38-39.

Mao Q, Chang, S.W., Pfeiffer, R.L., 2000: Influence of large-scale initial oceanic mixed layer depth on tropical cyclones. *Mon. Wea. Rev.,* **128,** 4058-4070.

Martin J.P., Rudnick D.L., 2007: Inferences and observations of turbulent dissipation and mixing in the upper ocean at the Hawaiian Ridge. *J. Phys. Oceanography,* **37,** 476-494.

Michaels P.J., Knappenberger, P.C., Davis R.E., 2006: Sea surface temperatures and tropical cyclones in the Atlantic basin. *Geophys. Res. Lett.,* **33,** L09708, DOI:10.1029/ 2006GL025757.

Pasquero C., and Emanuel, K. 2008: Tropical cyclones and transient upper-ocean warming. *J.Climate,* **21,** 149-162.

Pineda, J. , 1991: Predictable upwelling the shoreward transport of planktonic larvae by internal tidal bores, *Science,* **253**, 548-551.

Pineda, J., 1995: An internal tidal bore regime at nearshore stations along western U.S.A.: predictable upwelling within the lunar cycle, *Cont. Shelf Res.*, **15**, 1023-1041.

Rappaport, E.N., J.L. Franklin, L.A. Avila, S.R. Baig, J.L. Beven, E.S. Blake, C.A. Burr, J.G. Jiing, C.A. Juckins, R.D. Knabb, C.W. Landsea, M. Mainelli, M. Mayfield, C.J. McAdie, R.J. Pasch, C. Sisko, S.R. Stewart, and A.N. Tribble, 2009: Advances and Challenges at the National Hurricane Center, *Wea. Forecasting*, **24,** 395–419.

Schiller, A., and R. Fiedler, 2007: Explicit tidal forcing in an ocean general circulation model, *Geophys. Res. Lett., **34,** L03611.

Sharples, J., P.M. Holligan, J. Tweddle, J. H. Simpson, T. P. Rippeth, and Palmer M., 2006: Spring-neap pulses of primary production in the seasonal shelf sea thermocline, *Geophys. Res. Abs.,* **8,** *03384.*

Shay L, Goni G, Black P., 2000: Effects of warm oceanic features on Hurricane Opal. *Mon. Wea. Rev.,***128,** 131–148.

Smiley C., 1954: Tidal forces and the formation of hurricanes. *Nature* **173:** 397.

Swain D, Ali MM, and Weller RA. 2006. Estimation of mixed-layer depth from surface parameters. *J. Marine. Res.,* **64,** 745-758*.*

Thorpe, S.A., 2005: The Turbulent Ocean, 439 pp., Cambridge University Press, Cambridge, UK.

Visvanathan, T.R., 1966: Formation of depressions in the Indian Seas and Lunar Phase. *Nature* , *210*, 406-407*.*

Zar, J. H., 1984: *Biostatistical Analysis*, *2nd ed.*, 718 pp., Prentice-Hall, Englewood Cliffs, New Jersey.
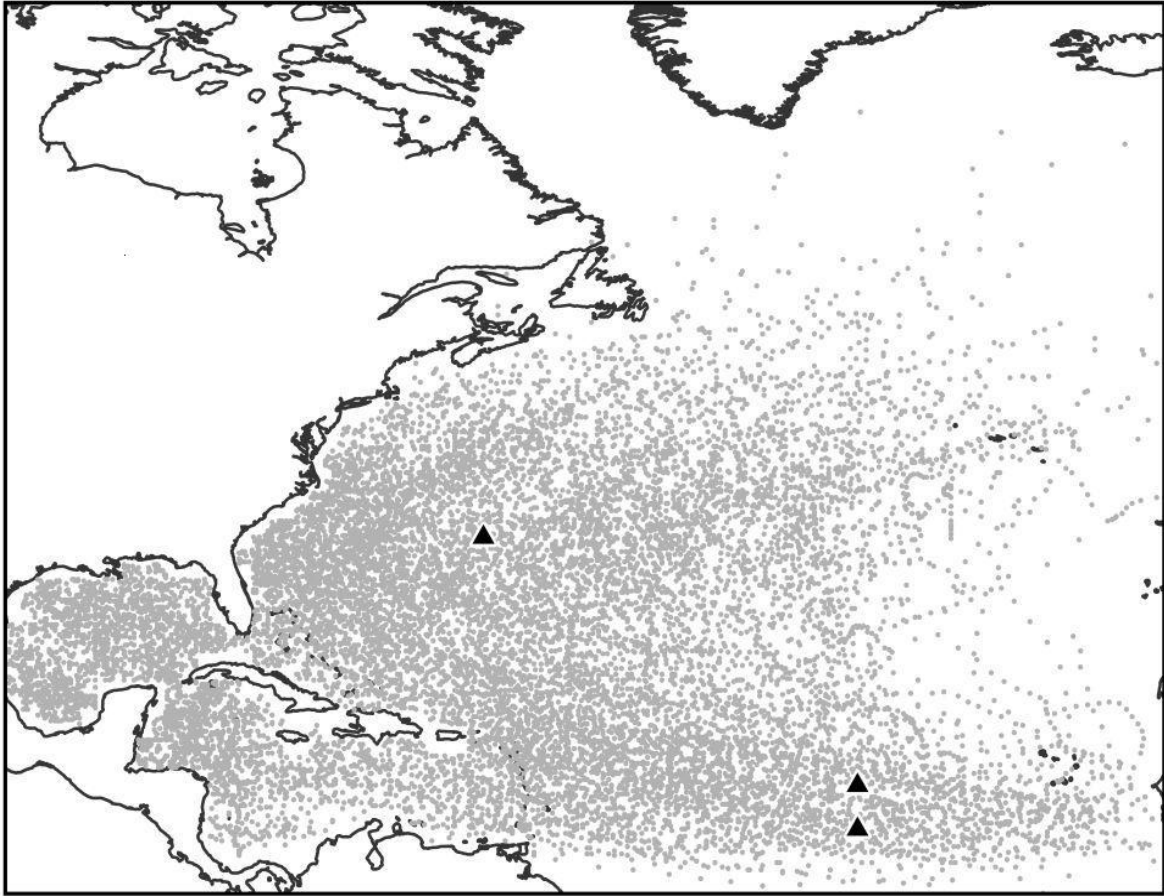
Figure One. Map of study area showing locations of moorings (triangles). Gray denotes

HURDAT observations used in the study.
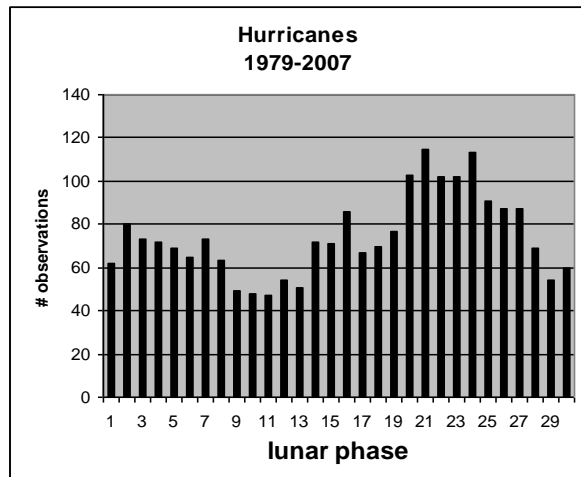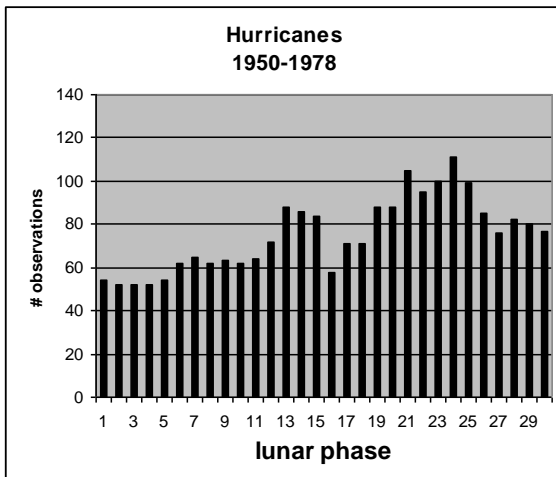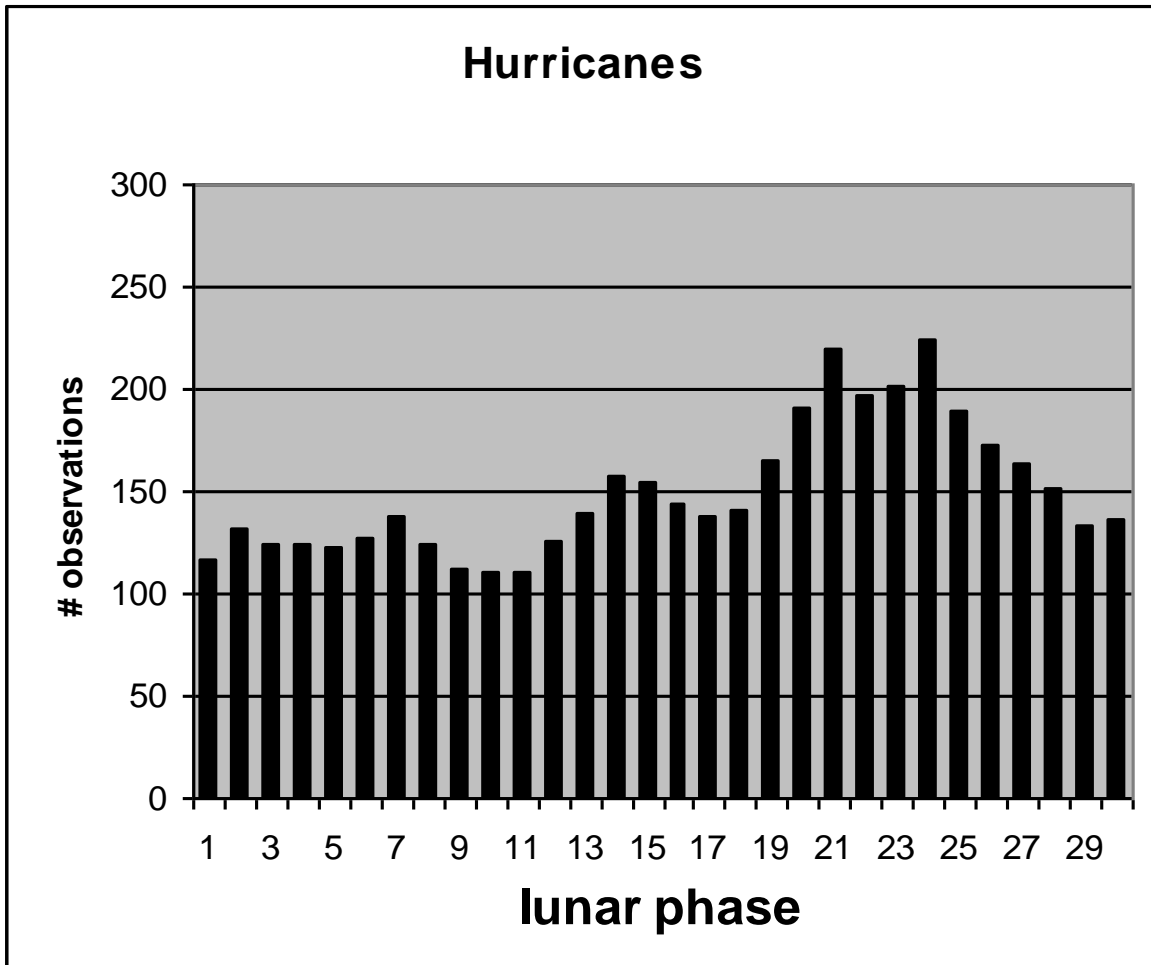
Figure Two. Timing of hurricane occurrence (HURDAT observations) by lunar phase from 1950 to 2007, and separately in the first and second halves of this study period.
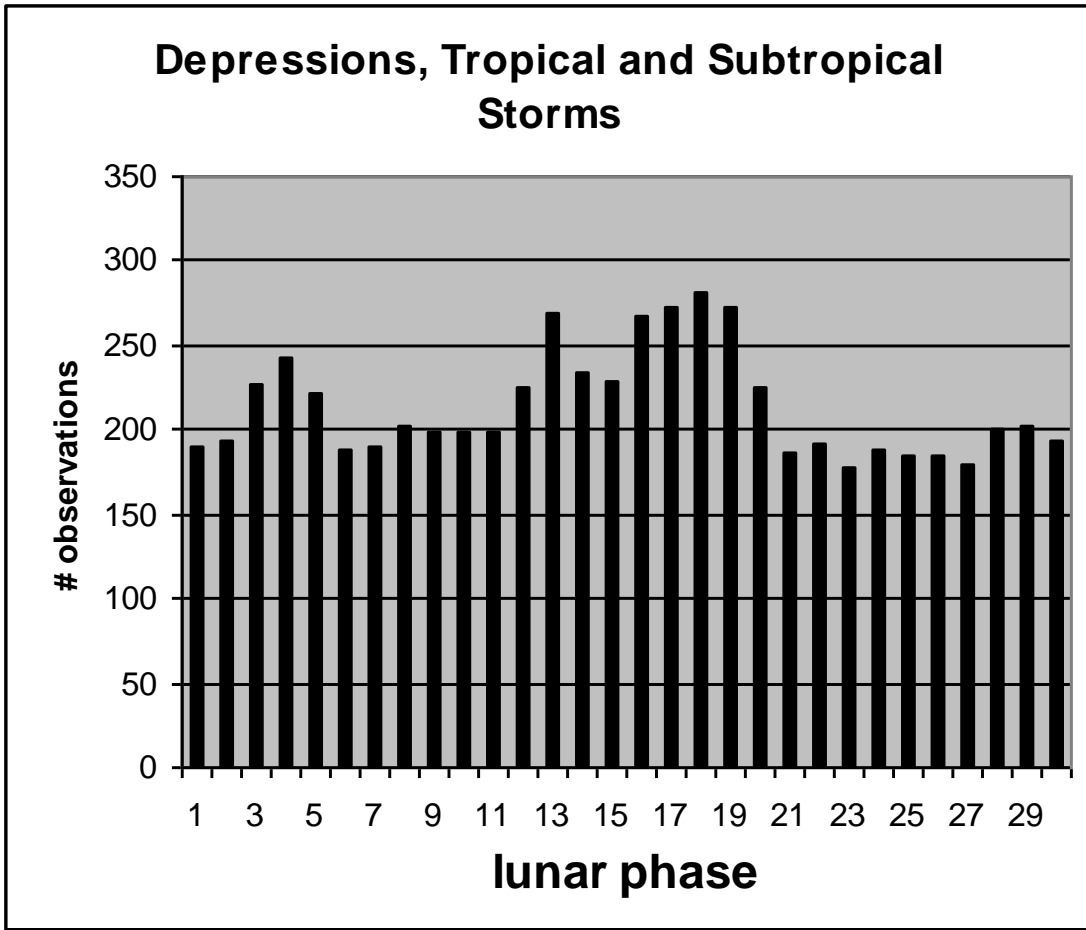
Figure Three. Timing of tropical depressions, and tropical and subtropical storms
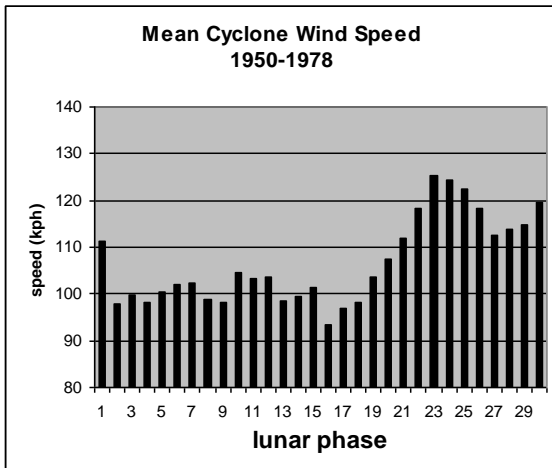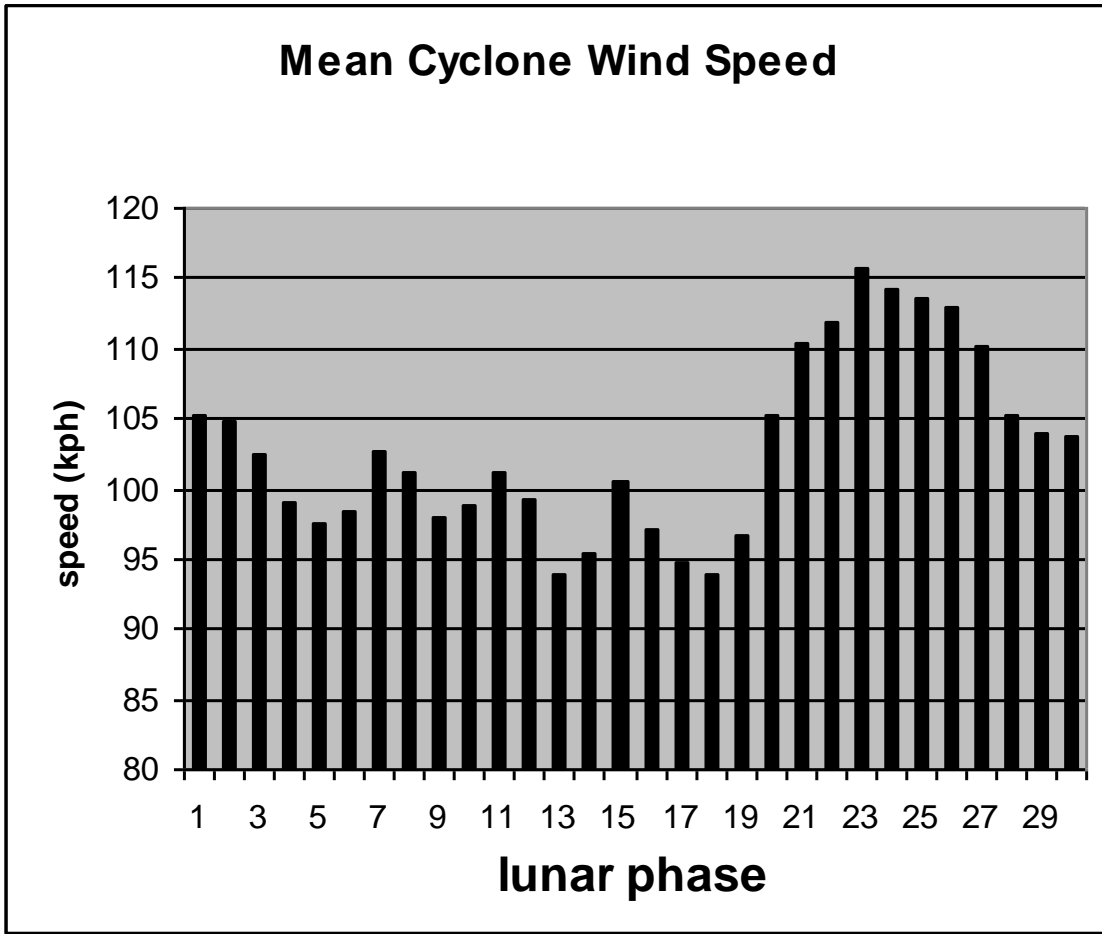
(HURDAT observations) by lunar phase from 1950 to 2007
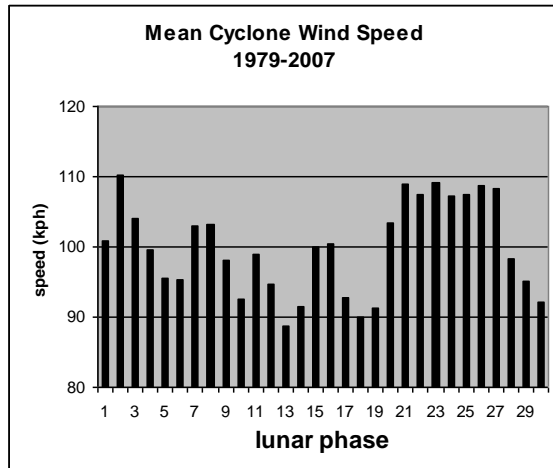
Figure Four. Tropical cyclone wind speeds in relation to the lunar synodic cycle from 1950 to 2007, and separately in the first and second halves of this study period.
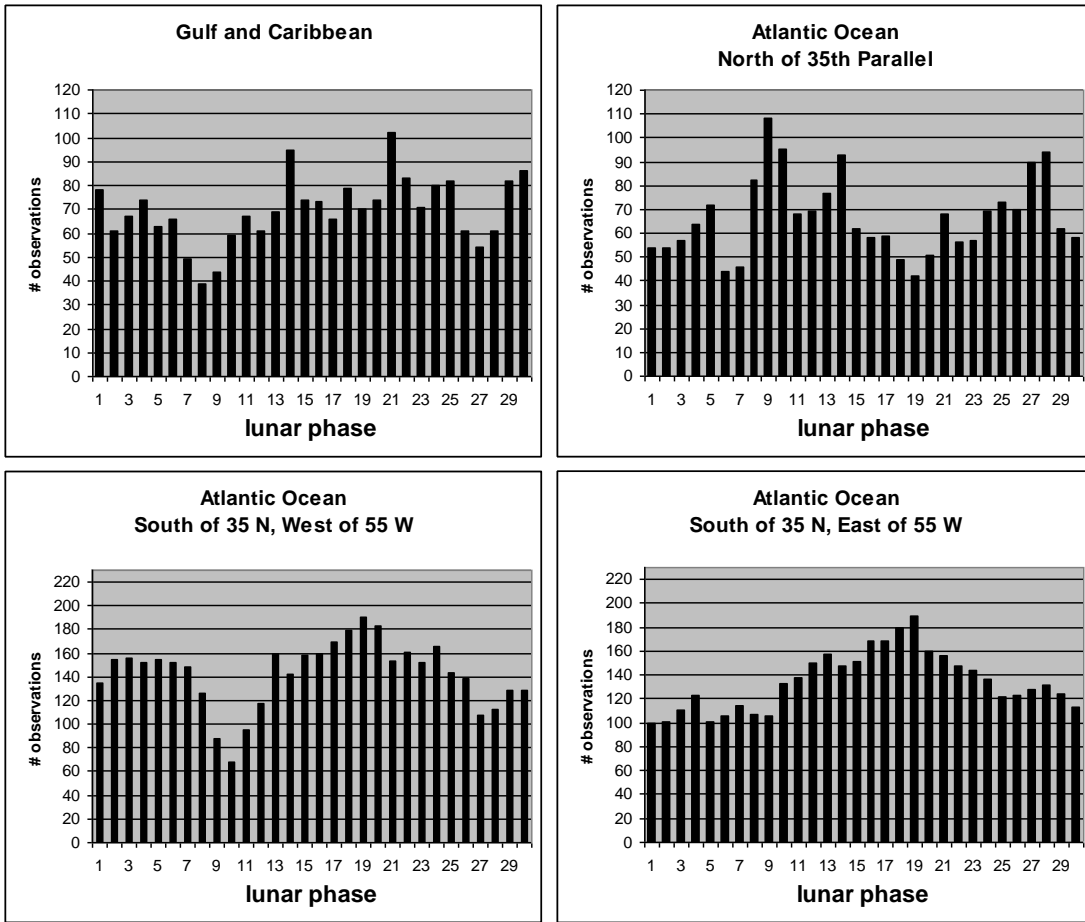
Figure Five. Tropical cyclone observations in four subdivisions of the Atlantic Ocean, in relation to the lunar synodic cycle.
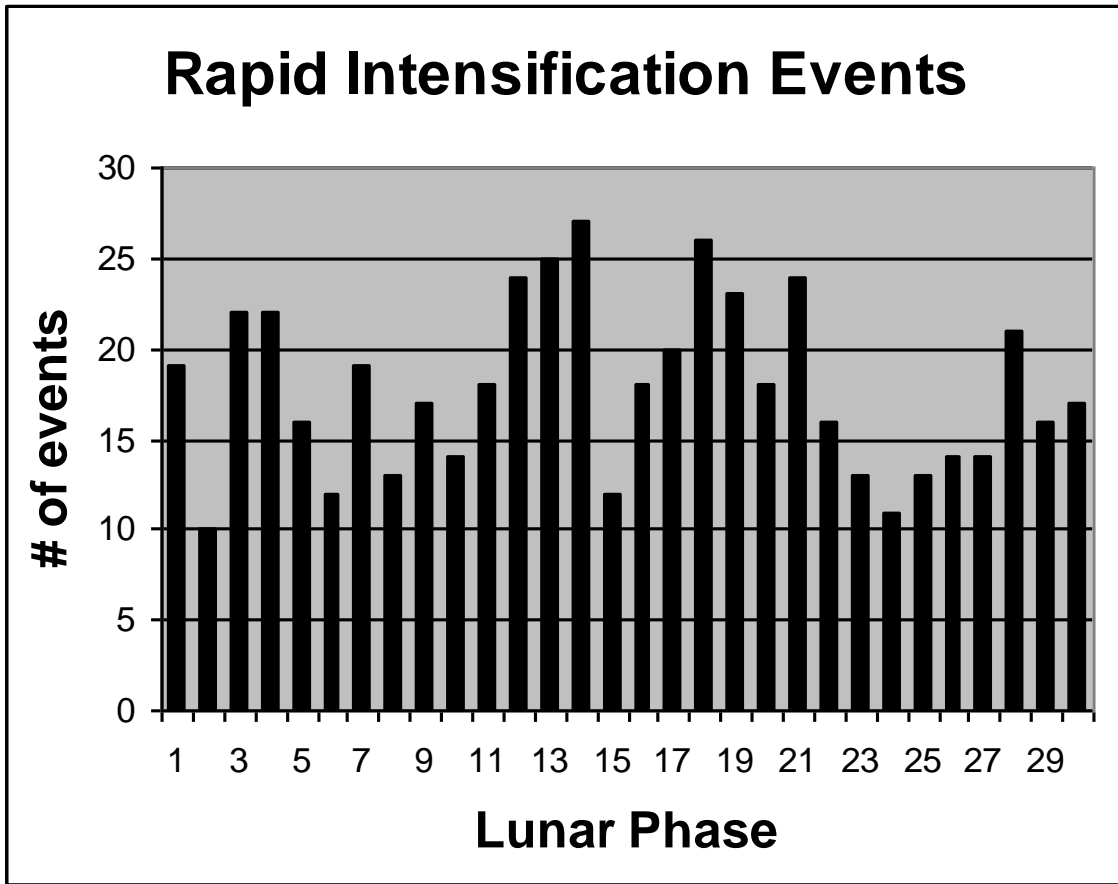
Rapid Intensification Events

Figure Six. Timing of onset of rapid intensification events for Atlantic tropical cyclones in relation to the lunar synodic cycle.

12N 38W PIRATA Mooring

mean temperature vs lunar phase

15N 38W PIRATA Mooring

mean temperature vs lunar phase
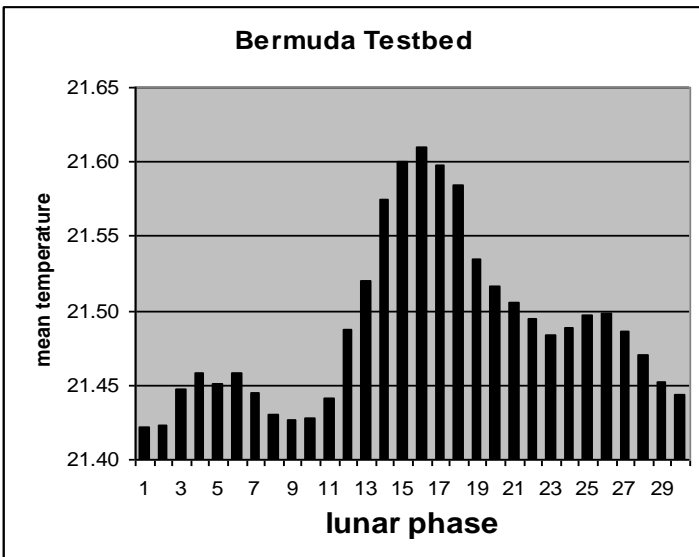
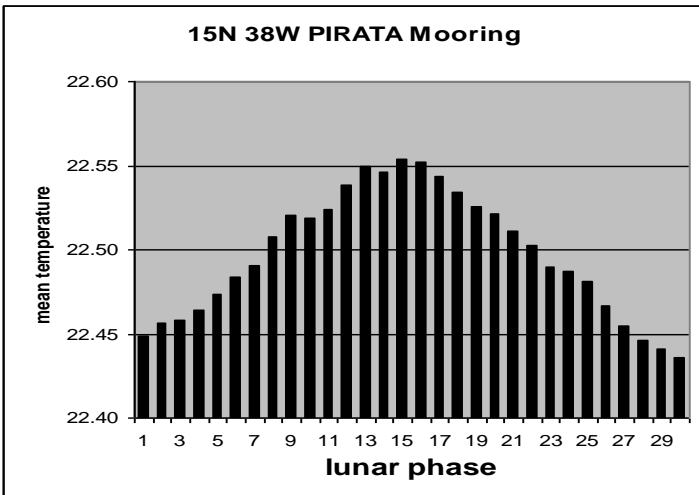## Bermuda Testbed

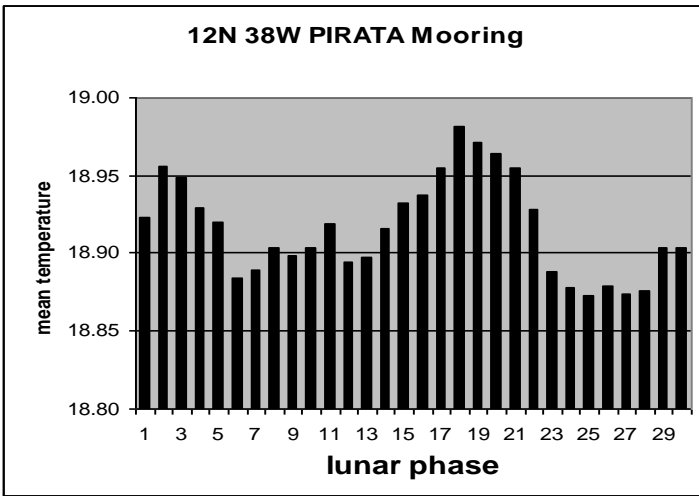mean temperature vs lunar phase

Figure Seven. Mean ocean temperatures at sensor depths between 35-150 m at three ocean

moorings, in relation to the lunar synodic cycle.